Targeting of the Yeast Plasma Membrane [H+]ATPase: A Novel Gene *ASTI* Prevents Mislocalization of Mutant ATPase to the Vacuole

Amy Chang and Gerald R. Fink

Whitehead Institute for Biomedical Research, Cambridge, Massachusetts 02142

Abstract. We have characterized a class of mutations in *PMA1*, (encoding plasma membrane ATPase) that is ideal for the analysis of membrane targeting in *Saccharomyces cerevisiae*. This class of *pma1* mutants undergoes growth arrest at the restrictive temperature because newly synthesized ATPase fails to be targeted to the cell surface. Instead, mutant ATPase is delivered to the vacuole, where it is degraded. Delivery to the vacuole occurs without previous arrival at the plasma membrane because degradation of mutant ATPase is not prevented when internalization from the cell surface is blocked. Disruption of *PEP4*, encoding vacuolar proteinase A, blocks ATPase degradation, but fails to restore growth because the ATPase is still improperly targeted.

One of these *pma1* mutants was used to select multicopy suppressors that would permit growth at the nonpermissive temperature. A novel gene, *ASTI*, identified by this selection, suppresses several *pma1* alleles defective for targeting. The basis for suppression is that multicopy *ASTI* causes rerouting of mutant ATPase from the vacuole to the cell surface. *pma1* mutants deleted for *ASTI* have a synthetic growth defect at the permissive temperature, providing genetic evidence for interaction between *ASTI* and *PMA1*. Astl is a cytoplasmic protein that associates with membranes, and is localized to multiple compartments, including the plasma membrane. The identification of *ASTI* homologues suggests that Astl belongs to a novel family of proteins that participates in membrane traffic.

THE plasma membrane mediates interaction between the cell and the extracellular environment. To maintain the unique identity and function of this organelle, it is essential that newly synthesized plasma membrane proteins are accurately sorted and targeted. Defects in intracellular transport and cell surface expression of plasma membrane proteins, including ion transporters and channels, are well-known causes of human disease (Amara et al., 1992; Ashcroft and Roper, 1993).

Proteins destined for the cell surface enter the secretory pathway at the ER. Folding and assembly of newly synthesized proteins at the ER is promoted by molecular chaperones that interact selectively with nascent polypeptides (Gething and Sambrook, 1992; Bergeron et al., 1994; Shinde et al., 1993). Chaperones comprise one component of a quality control mechanism functioning at the ER (Klausner, 1989). This quality control system prevents the export of misfolded and improperly assembled proteins, and it degrades retained proteins (Klausner and Sitia, 1990). Since assembly of at least one integral plasma membrane protein occurs after exit from the ER, quality control may occur at multiple steps of the secretory pathway (Musil and Goodenough, 1993). Thus, the requirements for transit through the secretory pathway may be unique for individual proteins. For example, amino acid permeases in yeast require a novel gene, *SHR3*, for transport from the endoplasmic reticulum (Ljungdahl et al., 1992). Analogously, a specific receptor is required exclusively for targeting of carboxypeptidase Y to the vacuole (Marcusson et al., 1994).

Newly synthesized proteins move from the ER to the Golgi, where proteins destined for the lysosome/vacuole are sorted from those destined for the cell surface. Vacuole-bound proteins transit through endosomes, which lie at the intersection between biosynthetic traffic and membrane internalized from the cell surface (Stack and Emr, 1993; Davis et al., 1993). In mammalian cells, transport to the plasma membrane is thought to occur by default, and delivery to or retention within other compartments of the secretory pathway is mediated by specific information contained in sorted proteins (Pfeffer and Rothman, 1987). In yeast, by contrast, it has recently been proposed that default membrane traffic is routed to the vacuole (Stack and Emr, 1993; Nothwehr and Stevens, 1994). This model is based on observations that resident Golgi membrane proteins are delivered to the vacuole when they are overexpressed or when specific retention signals are removed (Roberts et al., 1992; Nothwehr et al., 1993). A corollary of this model is that plasma membrane proteins in yeast are delivered to the cell surface because they have targeting signals that interact with specific receptors.

Address all correspondence to Amy Chang, Department of Anatomy and Structural Biology, Albert Einstein College of Medicine, 1300 Morris Park Avenue, Bronx, NY 10461. Tel.: (718) 430-2739. Fax: (718) 518-7236.

The plasma membrane [H+]ATPase of *Saccharomyces cerevisiae*, encoded by *PMA1* (Serrano et al., 1986), presents an excellent model for targeting studies because it is a major component of the cell surface, making up 10–20% of the total plasma membrane protein. Pma1 is predicted to have a polytopic membrane topology with 10 transmembrane segments, a large cytoplasmic domain containing ATP-binding and catalytic phosphorylation sites, and ~4% of the protein is extracytoplasmic (Serrano et al., 1986). Newly synthesized Pma1 is delivered to the plasma membrane via the secretory pathway, and its intracellular transport is accompanied by kinase-mediated phosphorylation on multiple Ser and Thr residues (Chang and Slayman, 1991). At the cell surface, the ATPase is quite stable with a half-life of ~11 h (Benito et al., 1991).

The plasma membrane [H+]ATPase belongs to the superfamily of P-type ion transporters, with which it shares structural and functional similarity (Gaber, 1992). By pumping protons out of the cell, the plasma membrane ATPase regulates cytoplasmic pH and creates the electrochemical proton gradient that drives nutrient uptake (Serrano et al., 1986; Gaber, 1992). ATPase activity is modulated by a variety of environmental factors, including glucose metabolism (Eraso and Portillo, 1994; Chang and Slayman, 1991) and acidification of the medium (Eraso and Gancedo, 1987). The *PMA1* gene is regulated transcriptionally (Garcia-Arranz et al., 1994; Kuo and Grayhack, 1994) and, because of its critical physiological role, its function is essential for viability.

Other members of the P-type ATPase family, e.g., the mammalian Na^+,K^+ and H^+,K^+ ATPases, have a β subunit whose assembly with the catalytic subunit is required for plasma membrane delivery and stability of the complex (Renaud et al., 1991; Jaunin et al., 1993; Eakle et al., 1994). The β subunit is a glycosylated transmembrane polypeptide with highly conserved structure; however, a subunit of this type has not been found for the yeast plasma membrane [H+]ATPase.

In this study, we have characterized temperature-sensitive *pma1* mutants that undergo growth arrest when ATPase protein and activity become limiting. We find that newly synthesized ATPase in these cells is defective for delivery to the plasma membrane and is, instead, degraded in the vacuole. We used the *pma1*^{ts} mutants as a basis for selection of genes involved in quality control and plasma membrane targeting. We identified *AST1*, a multicopy suppressor of temperature-sensitive growth of *pma1* cells, which reroutes mutant ATPase from the vacuole to the plasma membrane.

Materials and Methods

Strains and Media

Standard yeast media and genetic manipulations were as described in Sherman et al. (1986). Mutations in *PMA1* were made in vitro by hydroxylamine mutagenesis and transformed into yeast containing a deletion of *PMA1* on the chromosome and a functional *PMA1* copy on a plasmid. Temperature-sensitive yeast were isolated by plasmid shuffle (Boeke et al., 1987). *pma1-7* and *pma1-8* were cloned into pRS306 (Sikorski and Hieter, 1989) as 5-kb HindIII fragments to generate pAC7 and pAC8. The plasmids were linearized with BstEII, and *pma1-7* (ACY7) and *pma1-8* (ACY8) were integrated into the genome of strain L3852 (Antebi and Fink, 1992), replacing *PMA1* by pop-in, pop-out gene replacement. *AST1*-disrupted strains were constructed by transformation of diploid strains ACX7 (PMA1/*pma1-7*) with pAC19 and ACX24 with pAC69. Strains ACX7 and ACX24 were from crosses between ACY7 and L3854, and L3852 and L4364, respectively. Temperature-sensitive *pma1 sec* double mutants were derived from crosses between ACY7 and L5077 (Mat a *sec18-1 leu2-3,112 lys2Δ201 ura3-52*) and L5435 (Mat a *sec6-4 his 3Δ200 ade2 leu2-3,112 ura3-52*) (Antebi and Fink, 1992). The *pma1-7 end3-1* strain came from a cross between ACY7 and RH266-1D (Mat a *end3-1 leu2 his4 ura3 bar1-1*) (Raths et al., 1993). A list of the strains and plasmids used in this work are shown in Table I. Yeast transformations were performed by the lithium acetate method (Gietz et al., 1992).

Metabolic Labeling, Immunoprecipitation, Western Blot and ATPase Assay

Cultures were grown overnight in synthetic complete medium without methionine and uracil. Mid-log cells were harvested and resuspended in fresh medium. Temperature-sensitive mutants were shifted to 37°C for 5 min (except as noted) before pulse labeling for 2 min with Expre^{35}S^{35}S (New England Nuclear, Boston, MA) at 2 mCi/25 OD_{600} cells. An equal volume of complete medium plus 20 mM cysteine and methionine was added to start the chase. At various times of chase, aliquots were placed on ice in the presence of 10 mM Na azide and 2 mg/ml cycloheximide. Cell lysis and immunoprecipitation in RIPA buffer were as previously described (Chang and Slayman, 1991). Immunoprecipitations were normalized to acid-precipitable cpm, and analyzed by SDS-PAGE and autoradiography or phosphorimaging with a Fujix Bas2000 bioimage analyzer. Rabbit polyclonal anti-ATPase antibody was from Carolyn Slayman (Yale University, New Haven, CT). Anti-c-*myc* mouse monoclonal ascites fluid 9E10 was from Harvard University Cell Culture Facility (Boston, MA). For Western blot analysis and ATPase assays, samples were normalized to lysate protein as measured by Bradford (1976). For quantitative immunoblots, ^{125}I protein A (Amersham Corp., Arlington Heights, IL) was used to detect the primary antibody; otherwise, immune complexes were visualized with horseradish peroxidase-conjugated secondary antibodies (Jackson ImmunoResearch Laboratories, Inc., West Grove, PA) and chemiluminescence detection reagents (ECL Western blotting detection system; Amersham). For ATPase assays, total membranes were prepared by centrifugation of lysate at 100,000 *g* for 1 h. Membranes were resuspended in buffer containing 250 mM sucrose, 20 mM Hepes, pH 7.5, and vanadate-sensitive ATPase activity was assayed in the presence and absence of 100 μM vanadate, as described (Chang and Slayman, 1991).

Indirect Immunofluorescence

Immunofluorescent staining of cells was done essentially as described (Rose et al., 1990). For ATPase staining, mid-log cultures were shifted to 37°C for 1 h, before fixation with 4.4% formaldehyde in 0.1 M K phosphate, pH 6.5, for 2 h at room temperature. Cells were permeabilized with methanol and acetone before staining with affinity-purified rabbit anti-ATPase antibody or mouse anti-*myc* ascites fluid, followed by a Texas red- or Cy3-conjugated secondary antibody (Jackson ImmunoResearch Laboratories).

Plasmid Construction and Molecular Biology Techniques

High copy suppressors of *pma1-7* cells were isolated by transforming ACY7 with a yeast 2μ library (Connelly, C., and P. Hieter, personal communication). Plasmids were rescued from yeast transformants (Hoffman and Winston, 1987). A 2-kb XhoI-SacI fragment containing *AST1* was subcloned from pAC21 (the original isolate from the 2μ library) into centromeric and 2μ vectors (Sikorski and Hieter, 1989).

The *AST1* DNA sequence was determined by the dideoxy chain termination method (Sanger et al., 1977) using Sequenase (United States Biochemical Corp., Cleveland, OH). *AST1* was physically mapped to a locus between *CDC27* and *ILS1* on chromosome II by probing an ordered λ-based *S. cerevisiae* library (Riles et al., 1993). *AST2* sequence was provided by Fred S. Dietrich and David Botstein (*Saccharomyces* genome database, Stanford University, Stanford, CA.) *AST2* was cloned using PCR to amplify genomic DNA and to introduce restriction sites. The amplified 3-kb fragment containing *AST2* coding sequence and flanking sequences was digested with EcoRI and SacII and was cloned into pRS202 at EcoRI-SacII to generate pAC63.

Disruption of *PEP4* was accomplished by transformation with the 4.7-kb EcoRI-XhoI fragment of pAS173 (Sachs, A., unpublished data). *AST1* deletion plasmids were constructed by using PCR to amplify sequences from pAC21. pAC69 was constructed by cloning a 1.9-kb KpnI-BamHI PCR

Table I. Yeast Strains and Plasmids Used in This Study

Yeast Strain	Genotype	Source
L3852*	*Mat α his3Δ200 lys2Δ201 leu2-3,112 ura3-52 ade2*	Antebi and Fink (1992)
L3854	*Mat a/α his3Δ200/his3Δ200 lys2Δ201/lys2Δ201 leu2-3,112/leu2-3,112 ura3-52/ura3-52 ade2/ADE2 trp1-1/TRP1*	"
L4364*	*Mat a his3Δ200 lys2Δ201 leu2-3,112 ura3-52 ade2*	"
ACX24*	L4364 X L3852	This work
ACY7*	*pma1-7*	"
ACY8*	*pma1-8*	"
ACY12*	*pma1-7 PEP4::URA3*	"
ACX21-6D	*Mat a his3Δ200 lys2Δ201 leu2-3,112 ura3-52 ade2 pma1-7 sec18-1*	"
ACX18-4D	*Mat a his3Δ200 lys2Δ201 leu2-3,112 ura3-52 ade2 pma1-7 sec6-4*	"
ACX19-4A	*Mat a his3Δ200 leu2-3,112 ura3-52 ade2 pma1-7 end3-1*	"
ACX19-4C	*Mat a his3Δ200 lys2Δ201 leu2-3,112 ura3-52 end3-1*	"
ACX7-8A	*Mat a his3Δ200 lys2Δ201 leu2-3,112 ura3-52 ade2 pma1-7*	"
ACX7-8B	*Mat α his3Δ200 lys2Δ201 leu2-3,112 ura3-52 ade2 trp1-1*	"
ACX7-8C	*Mat α his3Δ200 lys2Δ201 leu2-3,112 trp1-1 ast1:URA3*	"
ACX7-8D	*Mat a his3Δ200 lys2Δ201 leu2-3,112 ast1:URA3*	"
ACX30-2B*	*Mat α ast1:URA3*	"
ACY21*	*pma1-7[pAC21]*	"
Plasmid		
pAC21	*AST1 URA3 2μ*	Original isolate from 2μ library
pAC22	*AST1 URA3 CEN*	This work
pAC49	*AST1 URA3 2μ*	"
pAC63	*AST2 URA3 2μ*	"
pAC56	*AST1::myc URA3 CEN*	"
pAC64	*AST1::myc³ LEU2 CEN*	"
pAC65	*AST1::myc³ URA3 2μ*	"
pAC69	*ast1:URA3* pBluescript	"
pAC19	*ast1:URA3* pBluescript	"

All strains marked with asterisks are isogenic with L3852.

product upstream of the *AST1* start codon and a 1.3-kb BamHI-SacII fragment downstream of the stop codon. pAC19 is like pAC69, except that the upstream fragment is 2.3 kb and includes 274 bp of *AST1* coding sequence. Disruptions were marked with a 5-kb BamHI-BglII fragment from plasmid B2178 containing *URA3*. Deletion of *AST1* was confirmed by Southern analysis.

For epitope-tagging Ast1, oligonucleotide-directed mutagenesis was used to introduce a BamHI site at +6 nucleotides after the ATG to generate pAC62. Plasmid pAC64 was generated by cloning the 200 bp BamHI fragment from plasmid B2768, into the BamHI site of pAC62, thereby introducing three tandem copies of a c-*myc* epitope between amino acid residues 2 and 3 of *AST1*. A single copy of the *myc* tag was introduced at the same position of *AST1* by using site-directed insertion mutagenesis (Kunkel et al., 1987).

Results

Three Temperature-sensitive pma1 Mutants Are Defective for ATPase Stability

We characterized three temperature-sensitive *pma1* mutants that are defective in plasma membrane ATPase stability. Temperature-sensitive mutations were identified by plasmid shuffle after in vitro mutagenesis of *PMA1* (Boeke et al., 1987). Two of the three mutations (*pma1-7* and *pma1-8*) were then integrated into the genome, replacing wild-type *PMA1*, by pop-in, pop-out gene replacement. As shown in Fig. 1 *A*, *pma1-7* cells grew at the permissive temperature (25°C or 30°C), but became growth-arrested at 37°C. This growth phenotype is reversible since the cells resumed growth when the plate was shifted back to the permissive temperature. Sequencing of the *pma1* mutation revealed two nucleotide changes in *pma1-7* resulting in changes at Pro434→Ala, lying near the conserved catalytic phosphorylation domain, and Gly789→Ser, predicted to lie in a cytoplasmic loop between transmembrane segments 8 and 9. Two additional alleles, *pma1-8* and *pma1-9*, caused similar temperature-sensitive growth arrest; *pma1-8* has a single change at Gly783→Ala, and *pma1-9* has two missense mutations at Pro198→Ser and Thr837→Ile. Fig. 1 *B* shows that the time course of growth arrest of *pma1-7* cells in liquid culture was slow, with the first detectable decrease in the growth rate occurring at ≥6 h after shifting the cells to 37°C.

Western blot analysis of the steady state level of ATPase protein revealed that *pma1-7* cells at the permissive temperature have ~30% of the ATPase protein of isogenic wild-type cells (Fig. 2 *A*). After a shift to 37°C, there was a dramatic loss of ATPase protein in *pma1-7* cells, with ~20% of that seen at 25°C remaining after 6 h (Fig. 2 *A*, *middle*, *a* vs *c*). Since newly synthesized ATPase is degraded in the mutant (see below), the ~20% remaining appears to represent dilution of preexisting surface ATPase, since the cells undergo about two doublings in 6 h. A similar loss of ATPase protein was observed when *pma1-8* and *pma1-9* cells were shifted to the restrictive temperature.

After 6 h at 37°C, vanadate-sensitive ATPase activity of *pma1-7* cells also decreased, although to a lesser extent than

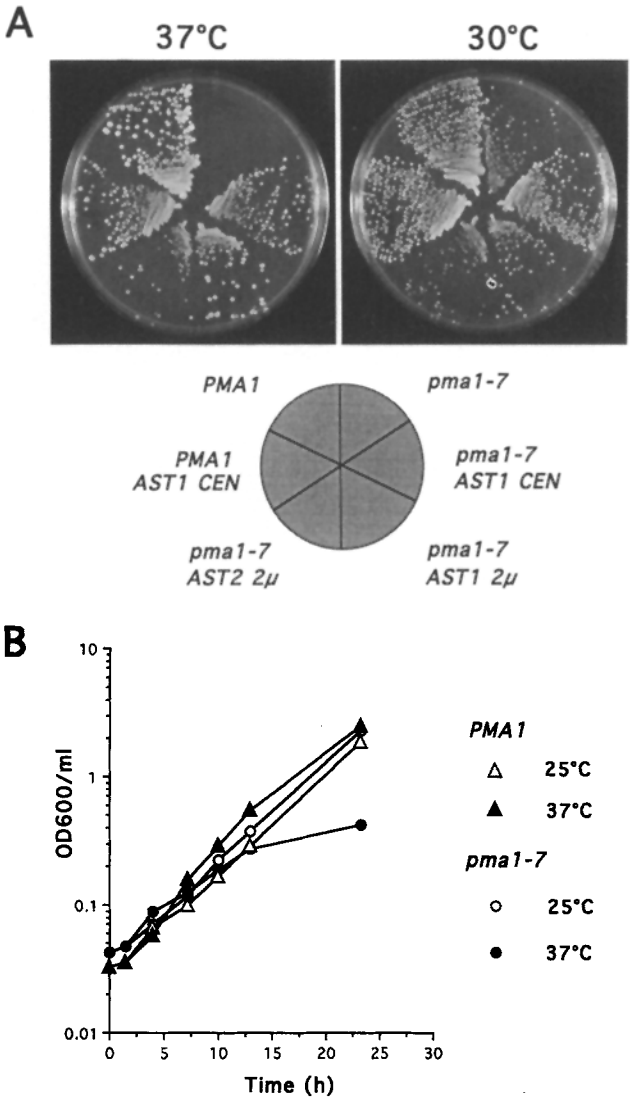

Figure 1. High copy *AST1* suppresses the growth arrest phenotype of *pma1-7* cells at 37°C. (*A*) Growth at 30°C and 37°C on plates (synthetic complete medium without uracil). Strains shown are L3852 (*PMA1*) bearing vector or pAC22 (*AST1 CEN*) and ACY7 (*pma1-7*) bearing vector, pAC22, pAC49 (*AST1* 2μ), or pAC63 (*AST2* 2μ). (*B*) Growth curve showing cell density (OD_{600}/ml) as a function of time at 25°C and 37°C in synthetic complete medium without uracil.

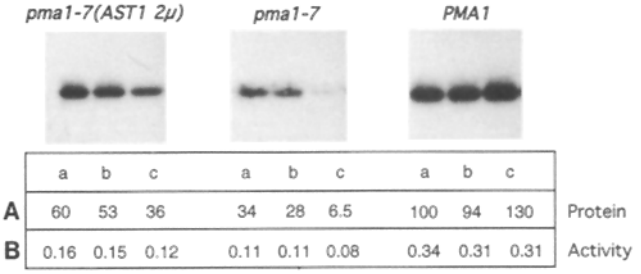

Figure 2. ATPase protein is degraded in *pma1-7* and stabilized in *pma1-7[AST1 2μ]* cells. (*A*) Western blot showing the steady-state level of ATPase protein. Lysate and total membranes were prepared from exponentially growing cells at 25°C (*a*), after an additional 6-h of growth at 25°C (*b*), and after 6 h at 37°C (*c*). Western blot samples were normalized to lysate protein. ATPase protein was detected using affinity-purified rabbit anti-ATPase antibody and ^{125}I-protein A and quantitated by phosphorimaging. ATPase protein is expressed relative to that seen in *PMA1* (*a*), set to 100 arbitrary units. (*B*) Vanadate-sensitive ATPase activity of total membranes expressed as micromoles per minute per milligram protein. (*Left*) *pma1-7[AST1 2μ]* (ACY21); (*middle*) *pma1-7* (ACY7); (*right*) *PMA1* cells (L3852).

ATPase protein (Fig. 2 *B*). Thus, the cells appear to upregulate the specific activity of the remaining Pma1. The slight drop in activity is in agreement with the time course of growth arrest (Fig. 1 *B*), and it suggests that ATPase activity eventually becomes rate limiting for growth. No drop in activity was observed in vitro when membranes isolated from mutant cells were shifted to 37°C, suggesting that ATP-driven catalysis by the mutant enzyme is not intrinsically thermosensitive. However, mutant ATPase is defective in intracellular transport and cell surface expression (see subsequent section).

AST1 Is a Multicopy Suppressor of pma1^{ts}

The *pma1* mutant was used as the basis for genetic selection of proteins involved in quality control and plasma membrane delivery. *pma1-7* cells were transformed with a multicopy yeast library (Connelly, C., and P. Hieter, unpublished data) and plated at 37°C. Plasmids were rescued from transformants that grew at 37°C. Several genes were isolated by this selection process, including *PMA1*. One of these genes, *AST1* (ATPase stabilizing), was chosen for further analysis because it suppressed the growth arrest phenotype of all three *pma1^{ts}* alleles, as well as two *pma1^{ts}* alleles previously characterized by Cid and Serrano (1988) [Ala547→Val and Gly254→Ser, but not Thr212→Ile or the double-mutant Asp91→Tyr, Glu92→Lys]. *pma1-7* cells could grow at 37°C when transformed with *AST1* on a multicopy 2μ plasmid or even on a low copy centromeric plasmid (Fig. 1 *A*).

Loss of mutant ATPase protein and activity was suppressed by multicopy *AST1*. Quantitation of Western blots showed that the steady-state level of ATPase protein at 25°C was increased in *pma1-7[AST1 2μ]* cells compared with *pma1-7* cells (Fig. 2, *left a* vs *middle a*). Furthermore, the presence of multicopy *AST1* decreased the loss of mutant ATPase protein after shifting to 37°C for 6 h (Fig. 2, *left*, *b* vs *c*). ATPase activity in membranes from *pma1[AST1 2μ]* cells was also increased, reflecting increased ATPase stability; multicopy *AST1* did not directly affect ATPase specific activity (Fig. 2 *B*). By contrast with *pma1-7* cells, shifting *PMA1* cells to 37°C had no effect on the steady-state ATPase level or ATPase activity (Fig. 2, *right*).

Newly Synthesized ATPase in pma1-7 Cells Is Degraded in the Vacuole

Loss of mutant ATPase could result either from degradation of preexisting ATPase from the cell surface or from degradation of newly synthesized ATPase. The slow time course of growth arrest (Fig. 1 *B*) and loss of steady-state ATPase (Fig. 2) supported the latter hypothesis. Indeed, pulse-chase experiments (Fig. 3 *A*) show that newly synthesized ATPase in the *pma1-7* mutant was degraded with a half-time of ~20 min

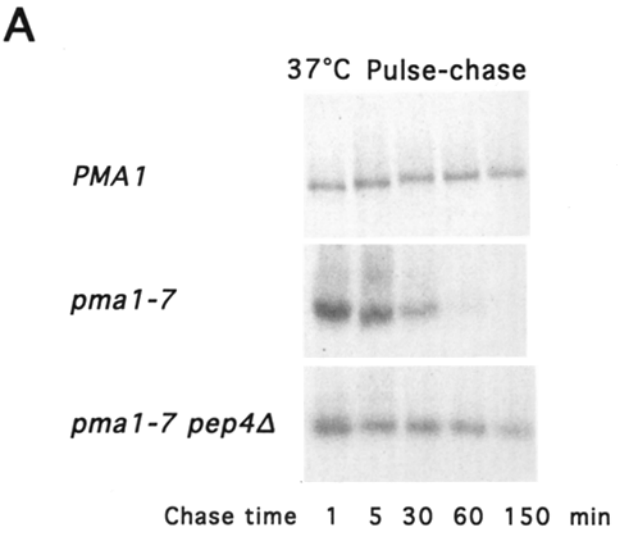

Figure 3. PEP4 disruption stabilizes newly synthesized ATPase, but it does not suppress growth arrest in *pma1-7*. (*A*) Degradation of newly synthesized ATPase in *pma1-7* cells is *PEP4*-dependent. Cells were shifted to 37°C for 5 min, pulse-labeled for 2 min with [^{35}S]Cys and Met, and chased for various times, as described in Materials and Methods. ATPase immunoprecipitation from cell lysates was normalized to acid-precipitable cpm. Immunoprecipitates were analyzed by SDS-PAGE and phosphorimaging. Pulse-chase analysis at 37°C of *PMA1* (L3852) cells (*top*); *pma1-7* (ACY7) cells (*middle*); *pma1-7 pep4* (ACY12) cells (*bottom*). (*B*) Growth on plates (synthetic complete) at 30°C and 37°C.

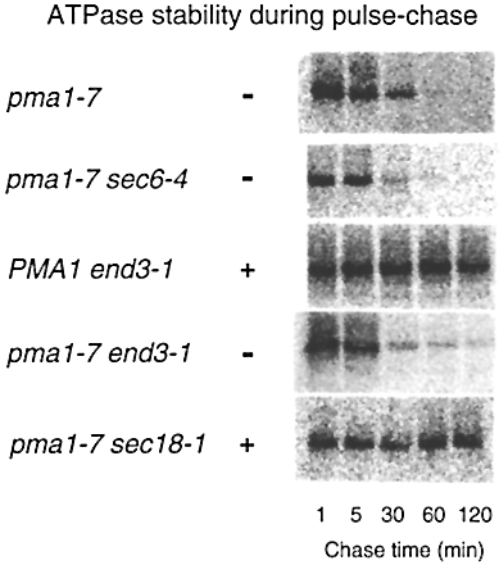

Figure 4. Newly synthesized mutant ATPase is degraded before delivery to the plasma membrane. Pulse-chase analysis of temperature-sensitive mutants at 37°C. (*Top to bottom*) *pma1-7* (ACY7); *pma1-7 sec6-4* (ACX18-4D); *PMA1 end3-1* (ACX 19-4C); *pma1-7 end3-1* (ACX19-4A); and *pma1-7 sec18-1* (ACX21-6D). *pma1-7* cells were shifted to 37°C for 5 min before labeling, while *end3-1* and *sec6-4* cells were shifted for 10 and 30 min, respectively.

at 37°C (*middle panel*). By contrast, wild type ATPase remained stable during the entire 2 h chase period (*top panel*).

Since delivery to the vacuole is a major pathway for protein degradation, we tested whether mutant ATPase was degraded in the vacuole by constructing a *pma1-7 pep4Δ* double mutant. Disruption of *PEP4*, encoding proteinase A, results in inactivation of vacuolar proteases (Jones, 1991). Pulse-chase analysis of *pma1-7 pep4Δ* cells showed stabilization of newly synthesized ATPase (Fig. 3 *A*, *lower panel*). Thus, degradation of newly synthesized ATPase is dependent on *PEP4*, and it is likely to occur in the vacuole. Importantly, although mutant ATPase was stabilized by *PEP4* disruption, the cells nevertheless were unable to grow at 37°C (Fig. 3 *B*). Therefore, ATPase stabilization by itself was not sufficient for growth.

Mutant ATPase Is Not Delivered to the Plasma Membrane, but It Goes Directly to the Vacuole

The pathway by which mutant ATPase is delivered to the vacuole for degradation was studied using a series of temperature-sensitive strains that are blocked in intracellular transport at discrete steps of the secretory pathway (Novick et al., 1981). Pulse-chase experiments showed stabilization of mutant ATPase by inhibition of export from the ER in *sec18-1* cells at 37°C (Fig. 4). By contrast, mutant ATPase is not stabilized by *sec6-4*, a mutation that results in inhibition of secretory vesicle fusion with the plasma membrane. Furthermore, when internalization from the cell surface was inhibited by *end3-1* (Fig. 4) or *end4-1* (not shown), no stabilization of newly synthesized mutant ATPase was seen. Since *end4-1* results in a temperature-sensitive block in endocytosis, whereas *end3-1* cells are defective in internalization at all temperatures (Raths et al., 1993), these data indicate that mutant ATPase is degraded before arrival at the plasma membrane.

Multicopy AST1 Stabilizes Mutant ATPase during Intracellular Transport

The idea that delivery to the vacuole occurs before arrival at the plasma membrane was further supported by the kinetics of degradation of newly synthesized ATPase. In Fig. 5 *A*, *pma1-7* cells were pulse labeled with [^{35}S]Cys and Met at 25°C, and were then shifted to 37°C at various times of chase. ATPase was immunoprecipitated, analyzed by SDS-PAGE, and quantitated by phosphorimaging. Even at the permissive temperature, a fraction of newly synthesized ATPase was degraded. The rate of degradation was increased when the cells were shifted from 25 to 37°C at 5 min of chase.

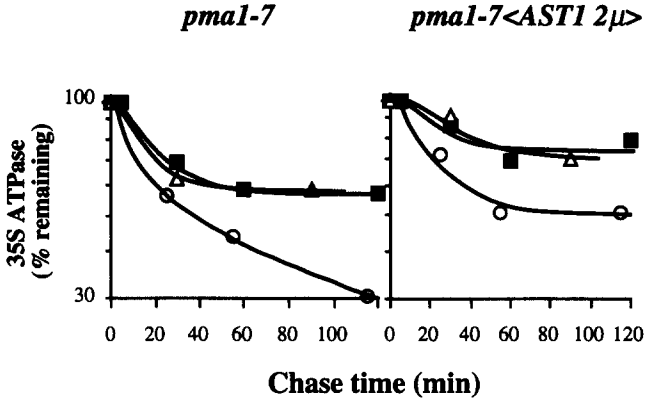

Figure 5. Degradation of newly synthesized mutant ATPase occurs at a discrete step during intracellular transport. *pma1-7* (ACY7) cells were pulse-labeled for 2 min with [^{35}S]Cys and Met, and chased at 25°C, as described in Materials and Methods. At 5 and 30 min of chase, aliquots were shifted to 37°C, and incubation continued. ATPase was immunoprecipitated from cell lysates, analyzed by SDS-PAGE, and quantitated by phosphorimaging. ATPase was normalized to that found at 5 min of chase at 25°C. (■) Chase at 25°C; (○) samples shifted to 37°C after 5 min of chase; (△) samples shifted to 37°C after 30 min of chase.

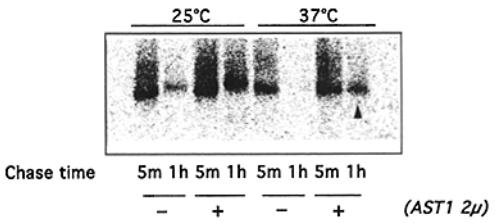

High copy *AST1* stabilizes newly synthesized ATPase

Figure 6. High copy *AST1* stabilizes newly synthesized mutant ATPase. Pulse-chase analysis of *pma1-7* cells with and without multicopy *AST1* (pAC21) at 25°C and 37°C. At 5 min and 1 h of chase, cells were lysed, and ATPase was immunoprecipitated, separated by SDS-PAGE, and analyzed by phosphorimaging. At 37°C, ATPase is stabilized by high copy *AST1*, but it does not undergo a mobility shift (*arrowhead*).

However, after 30 min of chase at 25°C, ATPase degradation was no longer increased by shifting to 37°C, i.e., increased ATPase degradation occurs at a specific interval during the chase. Thus, by ~30 min of chase, intracellular transport of mutant ATPase has progressed beyond the (Golgi) compartment from which delivery to the vacuole can occur.

In *pma1-7* cells overexpressing *AST1*, a 30-min chase at 25°C also allowed escape from increased ATPase degradation at 37°C. However, multicopy *AST1* decreased mutant ATPase degradation at all chase times (Fig. 5 *B*).

Fig. 6 shows an SDS polyacrylamide gel comparing the stability and electrophoretic mobility of newly synthesized ATPase in *pma1-7* cells in the absence and presence of multicopy *AST1*. Previous work has shown that wild-type ATPase undergoes a decrease in electrophoretic mobility during intracellular transport; the mobility change is caused by kinase-mediated phosphorylation, not glycosylation (Chang and Slayman, 1991). At 25°C, a shift in the electrophoretic mobility of mutant ATPase was seen during the chase in both the absence and presence of *AST1* (Fig. 6). At 37°C, phosphorylation of mutant ATPase appeared defective since the electrophoretic mobility was unchanged (Fig. 6, *arrowhead*). Nevertheless, multicopy *AST1* caused stabilization of mutant ATPase at 37°C.

Multicopy AST1 Reroutes Mutant ATPase from the Vacuole to the Plasma Membrane

Since growth arrest of *pma1* cells was suppressed by multicopy *AST1*, it seemed likely that *AST1* allows delivery of mutant ATPase to the cell surface. Indirect immunofluorescence showed that in wild-type cells (Fig. 7, *top*), ATPase staining was present over the cell surface and around the cell perimeter, characteristic of plasma membrane localization. To localize mutant ATPase, a *pep4Δ* strain was used to stabilize the protein. ATPase staining was predominantly intracellular in *pma1-7 pep4Δ* cells (Fig. 7, *middle*). Staining was coincident with vacuoles, visualized by Nomarski optics as depressions of the cell surface. The staining pattern confirms that mutant ATPase is delivered to the vacuole for degradation. Remarkably, in *pma1-7[AST1CEN]* cells, intracellular ATPase staining largely disappeared (Fig. 7 *A*, *bottom*); instead, the cells stained around the rim in a pattern similar to that seen in *PMA1* cells. Thus, ATPase localization in the presence of overexpressed *AST1* suggests a redistribution from the vacuole to the plasma membrane.

Molecular Characterization and Deletion of AST1

AST1 was cloned and sequenced. Physical mapping revealed that *AST1* lies on the left arm of chromosome II between *CDC27* and *ILS1*. The *AST1* open reading frame of 1,289 nucleotides predicts a 429–amino acid polypeptide (Fig. 8). The predicted polypeptide does not have an amino-terminal signal sequence nor any apparent transmembrane domains. Database searches revealed that *AST1* is 26% identical to an uncharacterized yeast open reading frame RF1095 on chromosome XIII (Behrens et al., 1991), and 70% identical to a second orf on chromosome V (Dietrich, F., and D. Botstein, unpublished data). The second orf has functional similarity to *AST1* since it was able, when expressed in high copy (pAC63), to suppress growth arrest of *pma1-7* (Fig. 1 *A*); it was named *AST2*. An alignment of the three genes is shown in Fig. 8. These data suggest that *AST1* belongs to a family of proteins with overlapping function.

Diploid strain ACX24 was transformed with the Asp718-SacII fragment of pAC69 to delete precisely the *AST1* open reading frame and replace it with a *URA3* marker. Sporulation and tetrad dissection resulted in four viable spores, 2:2 Ura$^+$:Ura$^-$ and growth of *PMA1* cells was not affected. A strain carrying deletion of both *AST1* and *AST2* was viable and displayed no growth defect. However, a synthetic growth defect was observed in *ast1Δpma1-7* cells at 30°C (Fig. 9 *A*), and the rate of ATPase degradation was increased in these cells (Fig. 9 *B*). Since one of the physiologic roles of Pma1 is to buffer cytosolic pH, the effect of buffering the medium was tested. Fig. 9 *A* shows that *ast1Δpma1* cells grew better in medium buffered to pH 5 when environmental stress and the demand for Pma1 was reduced (buffering the medium cannot, however, rescue *pma1^{ts}* cells from growth arrest at 37°C). The synthetic growth defect represents genetic evidence for interaction between *PMA1* and *AST1*.

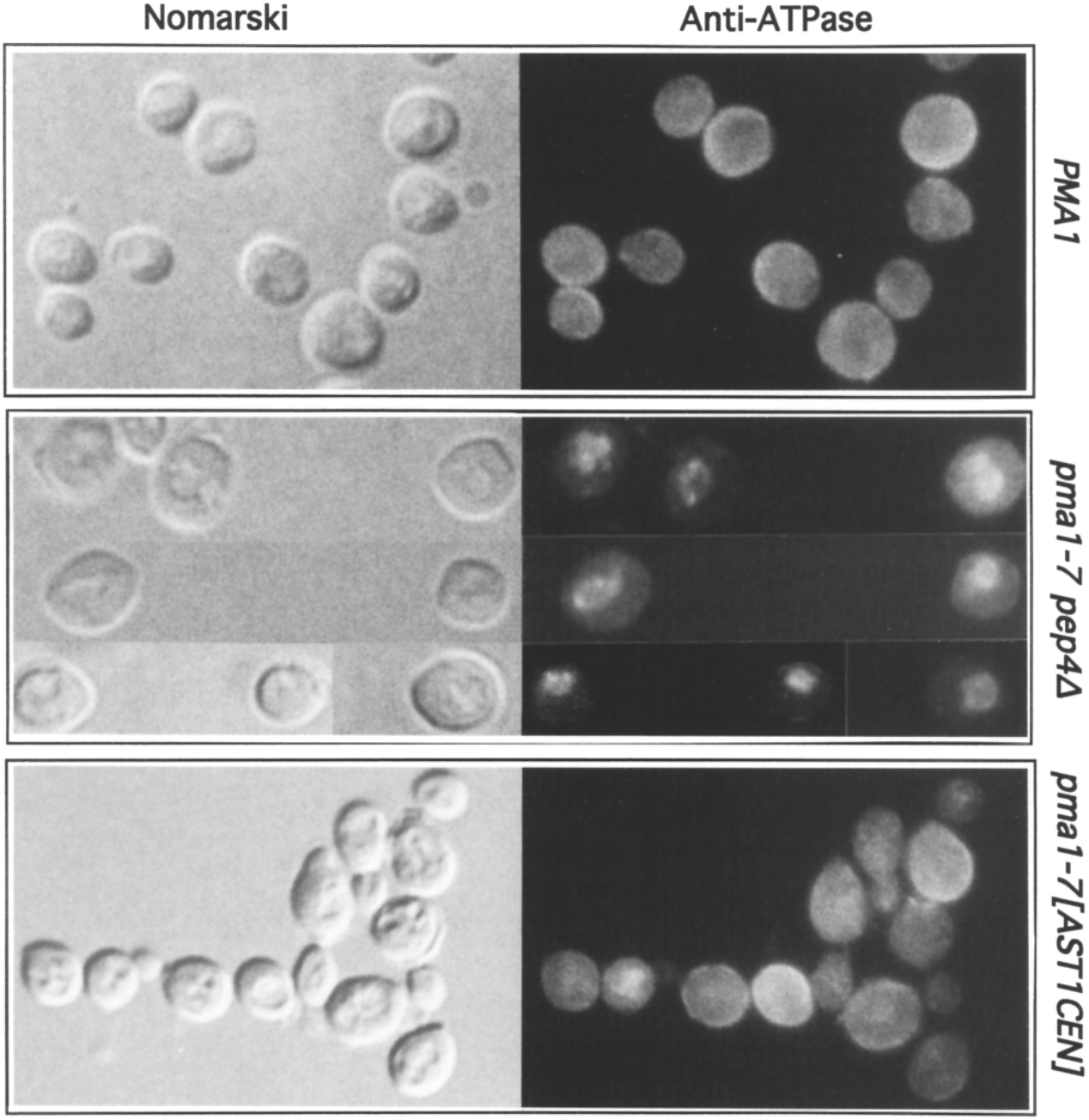

Figure 7. ATPase localization in *PMA1*, *pma1-7 pep4Δ*, and *pma1-7[AST1CEN]* cells. Nomarski imaging and indirect immunofluorescent localization of ATPase with polyclonal anti-ATPase antibody followed by Texas red–conjugated goat anti-rabbit IgG. Exponentially growing *pma1-7* (ACY7) cells bearing pAC22 (*AST1 URA3 CEN*), *pma1-7 pep4Δ* (ACY12) cells, and *PMA1* (L3852) bearing vector only, were harvested and resuspended in fresh synthetic complete medium without uracil. The cells were shifted to 37°C for 1 h before fixation. There is striking intracellular staining in *pma1-7 pep4Δ* cells, which overlies the vacuolar membrane (*middle panel*). The vacuole is seen by Nomarski optics as cell indentations. The majority of *pma1-7[AST1 CEN]* cells display a surface staining pattern, although some intracellular staining is also present.

Ast1 Protein Is Membrane-associated and Is Localized to Multiple Membrane Compartments

To characterize Ast1 further, a c-*myc* epitope was engineered at the amino terminus. Constructs with either a single copy or three tandem copies of the 11–amino acid epitope behaved as wild-type *AST1* in the ability to suppress growth arrest of *pma1*^{ts}. By Western blot (Fig. 10 *A*), *myc*-tagged Ast1 protein was visualized as a single band of M_r ~49 kD. Upon fractionation of cell lysate, essentially all Ast1 protein was associated with a 100,000-*g* membrane pellet. Consistent with the behavior of a peripheral membrane protein, Ast1 was progressively extracted into a soluble fraction with 0.5 M NaCl and 0.1 M Na carbonate, pH 11.5 (Steck and Yu, 1973). Ast1 was also insoluble in 1% Triton X-100, suggesting that it may be a part of a protein or lipid complex.

Indirect immunofluorescence was used to localize Ast1

Figure 8. Alignment of *AST1*, *AST2*, and a third homologous gene. Sequences were aligned with the Megalign program (DNAstar, Madison, WI) using the Clustal method (Higgins and Sharp, 1989). Identical amino acid residues are boxed and hyphens indicate gaps introduced to maximize alignment. *AST1* sequence is available from EMBL under accession number X81843. *AST2* sequence is unpublished data from F. Dietrich and D. Botstein (Stanford University, Stanford, CA). The peptide sequence for RF1095 is found in the SWISS-PROT protein sequence database under accession number P28625.

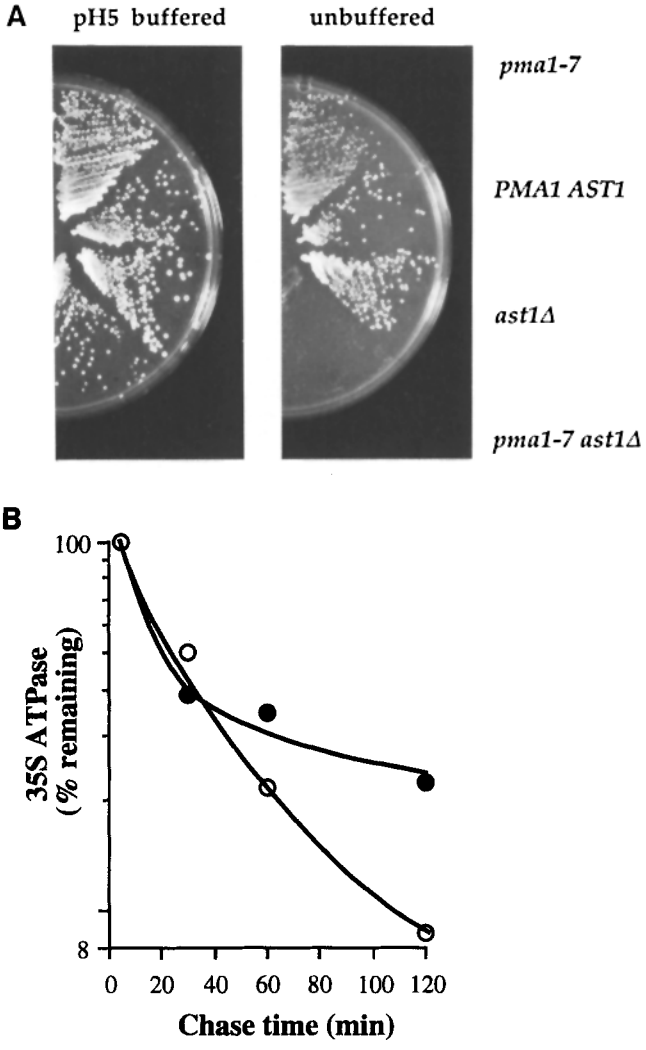

Figure 9. Synthetic growth defect of *ast1Δpma1-7* cells at 30°C. (*A*) Growth on plates with synthetic complete medium unbuffered or buffered to pH 5 with 50 mM Na citrate. Strains (ACX7-8A,B,C,D) are congenic ascospores. (*B*) Pulse-chase analysis of *pma1-7* (ACX7-8A) cells (●) and *pma1-7ast1::URA3* (ACX7-8D) cells (○) at 30°C.

protein. No staining with anti-*myc* antibody was seen in cells lacking the epitope-tagged construct (Fig. 10 *B*, *bottom*). A complex pattern was observed upon staining cells that express epitope-tagged Ast1 from a centromeric plasmid (Fig. 10 *B*, *top*). All cells showed punctate cytoplasmic staining that was excluded from the nucleus and vacuole. Staining around the perimeter was also seen in many cells (*arrows*). Strikingly, when Ast1 was expressed from a high copy 2μ plasmid, Ast1 distribution shifted so that staining was predominantly at the cell periphery, reminiscent of plasma membrane ATPase localization (Fig. 10 *B*, *middle*). These data suggest Ast1 is localized to cytoplasmic membranes, as well as to the plasma membrane.

Discussion

We have characterized a novel class of mutants that is defective for delivery of newly synthesized [H⁺]ATPase to the plasma membrane. Based on in vitro assay of ATP hydrolysis, the mutants do not appear to have substantially defective catalytic activity. Furthermore, the cells can grow if a fraction of newly synthesized ATPase is delivered to the cell surface at the permissive temperature (Fig. 6), or in the presence of multicopy *AST1* or several other *AST* genes. This behavior is similar to that observed for the temperature-sensitive ΔF508 mutant of the cystic fibrosis transmembrane conductance regulator, which is defective in intracellular transport but functional once delivered to the plasma membrane (Welsh and Smith, 1993). The slow time course of growth arrest of *pma1*^{ts} cells at 37°C is consistent with continuing function and a slow turnover rate of preexisting ATPase at the plasma membrane. A comparably slow time course of growth arrest is also observed when ATPase expression is shut off in cells where the *PMA1* is under the control of a galactose-dependent promoter (Cid et al., 1987).

Loss of mutant ATPase is caused by rerouting of the newly synthesized enzyme to the vacuole, based on indirect immunofluorescence localization of mutant ATPase (Fig. 7). This interpretation is further supported by pulse-chase experiments, which demonstrate ATPase stabilization in a *pep4Δ* mutant (Fig. 3). However, *PEP4* disruption causes ATPase stabilization without suppressing growth arrest,

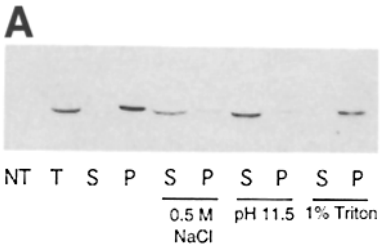

Figure 10. Characterization of Astl protein. (*A*) Astl protein is membrane-associated. Lysate of L3852 cells expressing epitope-tagged Astl (pAC56) was incubated on ice for 30 min with an equal volume of 1 M NaCl, 0.2 M Na carbonate, pH 11.5, or 2% Triton X-100. The lysate was then centrifuged at 100,000 *g* for 1 h to generate soluble and membrane fractions. The presence of Astl in total (*T*), supernatant (*S*), and pellet (*P*) fractions was detected by Western blot. No signal was seen in the absence of the epitope tag (*NT*). (*B*) Indirect immunofluorescence localization of epitope-tagged Astl with mouse anti-*myc* ascites fluid followed by Cy3-conjugated anti-mouse secondary antibody. *PMA1 astl*Δ cells (ACX30-2B) expressing myc-tagged *ASTI* from a centromeric plasmid (pAC64) are compared with cells (L3852) expressing myc-tagged *ASTI* 2μ (pAC65). 4′-6′ diaminophenylindole staining is shown on the right. No staining with anti-*myc* antibody was seen in cells without the epitope (*bottom panel*). Arrows indicate rim staining in some cells expressing *ASTI* from a centromeric plasmid.

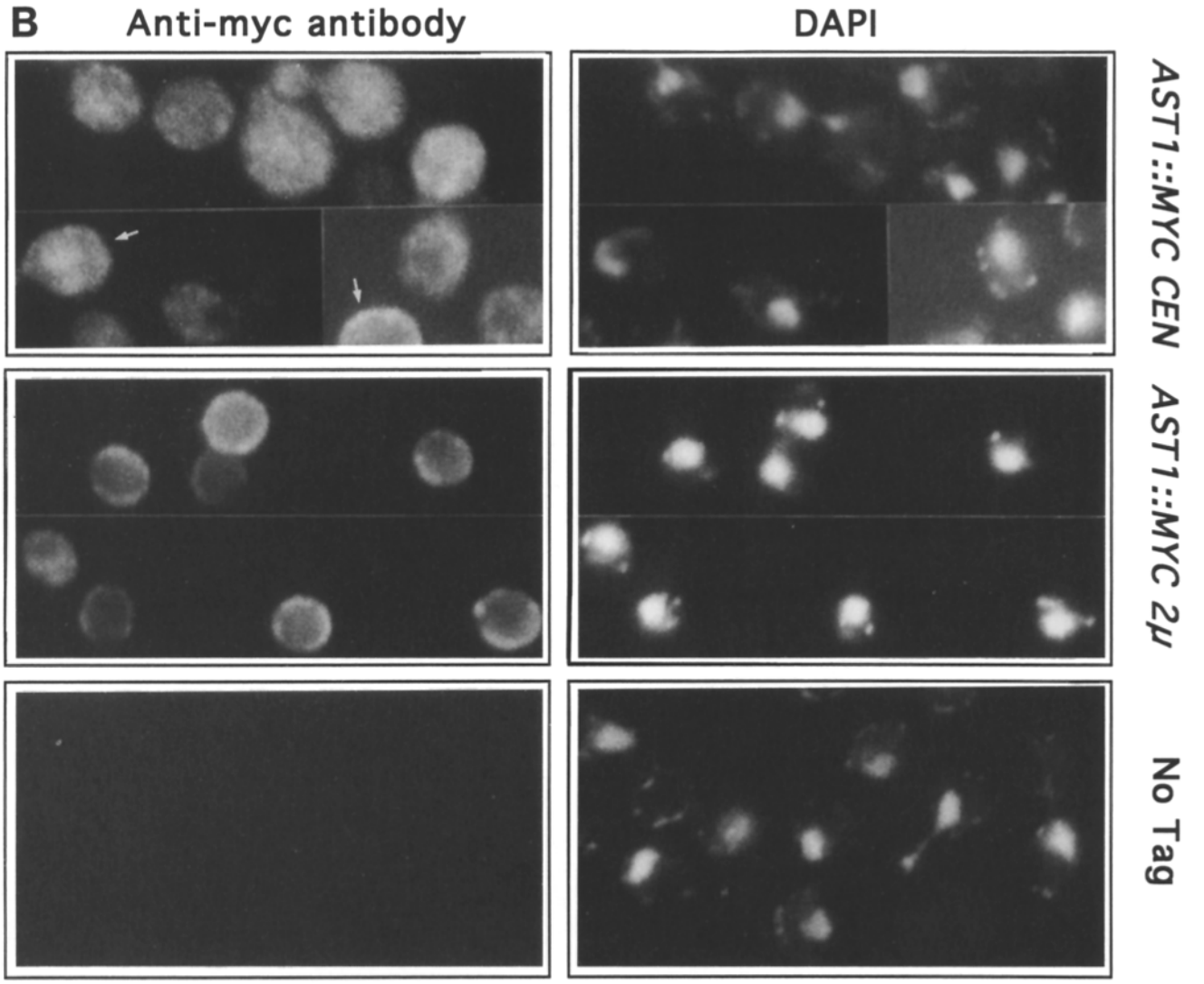

consistent with the idea that ATPase delivery to the plasma membrane is required for growth. Since the *end3* mutation, which blocks internalization from the cell surface, does not circumvent ATPase degradation (Fig. 4), it appears that delivery of mutant ATPase to the vacuole occurs without previous arrival at the plasma membrane. This conclusion is supported by the kinetics of ATPase degradation (Fig. 5), where newly synthesized ATPase was degraded during a specific interval of intracellular transport, and it was protected when transported beyond that step.

The behavior of the ATPase in temperature-sensitive *pma1* mutants bears directly on the mechanism of membrane protein transport in yeast. One model for the delivery of mutant ATPase to the vacuole is that it occurs by default. Recently, it has been proposed that delivery to the vacuole is the default pathway for membrane protein traffic in yeast (Stack and Emr, 1993; Nothwehr and Stevens, 1994), implying that cell surface membrane proteins in yeast have specific targeting signals. According to this model, mutant ATPase would be delivered to the vacuole because the plasma membrane targeting signal has been lost.

An alternative model is that defective proteins are spe-

cifically identified and targeted to the vacuole by a dedicated quality control mechanism. A mechanism for degradation of misfolded or unassembled proteins within the yeast ER has been reported (McCracken and Kruse, 1993), and some *pma1* mutants do accumulate ATPase at the ER (Harris et al., 1994). Although a mechanism for clearing unwanted cell surface proteins by endocytosis and subsequent degradation in the vacuole has been well characterized (Trowbridge et al., 1993; Davis et al., 1993), none has been uncovered for clearing defective plasma membrane proteins from the biosynthetic pathway by "direct" delivery to the vacuole. Nevertheless, the mutant ATPase described in this study is not the only example of a plasma membrane protein that is defective for cell surface delivery and is routed instead to the vacuole for degradation. In mammalian cells, a pentameric T cell receptor complex lacking 2 subunits is not efficiently transported to the plasma membrane, but is delivered instead to lysosomes (Minami et al., 1987). This observation is especially intriguing since most partial complexes and individual subunits of the T cell receptor are degraded at the ER (Klausner and Sitia, 1990). In addition, certain mutations in Ste3, the yeast a mating factor receptor, cause *PEP4*-dependent degradation without transport to the cell surface (Horecka, J., and G. Sprague, personal communication). At the present time, we cannot distinguish between default and quality control models for vacuolar delivery of mutant ATPase.

Overexpression of *AST1* stabilizes mutant ATPase protein, without directly affecting ATPase activity (Fig. 2). The mutant protein is stabilized because there is increased ATPase delivery to the plasma membrane (Fig. 7), and thus growth arrest is suppressed.

Based on our understanding of ATPase traffic in the *pma1* mutant, we reason that Ast1 must affect the ATPase at a step in intracellular transport before delivery to the vacuole, e.g., at the ER, Golgi, or endosome. Kinetic analysis indicates that mutant ATPase is stabilized by Ast1 at 30 min of chase (Fig. 5). Interestingly, newly synthesized ATPase moves into a Triton-insoluble fraction during intracellular transport (Chang, A., unpublished data), perhaps associating with Ast1, which is also Triton-insoluble. Ast1 behaves like a peripheral membrane protein and is localized to a cytoplasmic compartment(s), as well as to the plasma membrane (Fig. 10). These findings are consistent with a role for Ast1 in membrane traffic, in which it interacts with the cytoplasmic surface of one or more organelles of the secretory pathway, perhaps shuttling between cytoplasmic compartments and the plasma membrane.

Although *AST1* does not have sequence similarity with known chaperones, a simple model to explain how multicopy Ast1 allows cell surface delivery of mutant Pma1 is that Ast1 acts as a novel targeting/chaperone molecule. The synthetic growth defect seen in *pma1-7 ast1Δ cells* (Fig. 9) provides genetic evidence for interaction between Ast1 and Pma1. In addition, we have been able, under specific conditions, to coimmunoprecipitate Ast1 with the ATPase, supporting the idea that the two proteins may directly interact (Chang, A., unpublished data). Thus, Ast1 could facilitate delivery to the cell surface by interacting specifically with the ATPase.

Alternatively, Ast1 could play a general role in plasma membrane targeting as a component of the targeting machinery. Similar to a model that has been proposed for protein sorting in epithelial cells (Simons and Wandinger-Ness, 1990), Ast1 might participate in cell surface targeting by interacting with several plasma membrane proteins and lipids at the cytosolic side to form a subdomain that could bud to form a surface-directed vesicle. By either a specific or general model for Ast1 function, defective targeting of mutant ATPase would result from diminished interaction with Ast1.

Deletion of *AST1* and *AST2* did not significantly alter cell viability. The viability of the double-deletion strain is consistent with the hypothesis that there are additional members in the *AST* gene family. Future genetic and biochemical analyses should reveal the molecular mechanism for *AST* function in membrane traffic.

We thank John Teem for making the *pma1* mutants, and Fred Dietrich for providing the sequence of *AST2*; Peter Arvan, Harvey Lodish, David Pellman, and Daniel Kornitzer for comments on the manuscript; and members of the Fink lab for helpful discussions.

This work was supported by National Institutes of Health grant GM40266. A. Chang was supported by an academic research program grant from Merck Sharp & Dohme.

Received for publication 29 August 1994 and in revised form 10 October 1994.

References

Amara, J. F., S. H. Cheng, and A. E. Smith. 1992. Intracellular protein trafficking defects in human disease. *Trends Cell Biol.* 2:145–149.

Antebi, A., and G. R. Fink. 1992. The yeast Ca^{2+} ATPase homologue, PMR1, is required for normal Golgi function and localizes in a novel Golgi-like distribution. *Mol. Biol. Cell.* 3:633–654.

Ashcroft, F. M., and J. Roper. 1993. Transporters, channels, and human disease. *Curr. Opin. Cell Biol.* 5:677–683.

Behrens, M., G. Michaelis, and E. Pratje. 1991. Mitochondrial inner membrane protease 1 of *Saccharomyces cerevisiae* shows sequence similarity to the *Escherichia coli* leader-peptidase. *Mol. Gen. Genet.* 228:167–176.

Benito, B., E. Moreno, and R. Losario. 1991. Half-life of plasma membrane ATPase and its activating system in resting yeast cells. *Biochim. Biophys. Acta.* 1063:2645–268.

Bergeron, J. J. M., M. B. Brenner, D. Y. Thomas, and D. B. Williams. 1994. Calnexin: a membrane-bound chaperone of the ER. *Trends Biochem. Sci.* 19:124–128.

Boeke, J. D., J. Trueheart, G. Natsoulis, and G. R. Fink. 1987. 5-fluoroorotic acid as a selective agent in yeast molecular genetics. *Methods. Enzymol.* 154:164–175.

Bradford, M. 1976. A rapid and sensitive method for the quantification of microgram quantities of protein utilizing the principle of protein-dye binding. *Anal. Biochem.* 72:248–254.

Chang, A., and C. W. Slayman. 1991. Maturation of the yeast plasma membrane [H^+]ATPase involves phosphorylation during intracellular transport. *J. Cell Biol.* 115:289–295.

Cid, A., R. Perona, and R. Serrano. 1987. Replacement of the promoter of the yeast plasma membrane ATPase gene by a galactose-dependent promoter and its physiological consequences. *Curr. Genet.* 12:105–110.

Cid, A., and R. Serrano. 1988. Mutations of the yeast plasma membrane H^+-ATPase which cause thermosensitivity and altered regulation of the enzyme. *J. Biol. Chem.* 263:14134–14139.

Davis, N. G., J. L. Horecka, and G. F. Sprague, Jr. 1993. *Cis-* and *trans*-acting functions required for endocytosis of the yeast pheromone receptors. *J. Cell Biol.* 122:53–65.

Eakle, K. A., M. A. Kabalin, S.-G. Wang, and R. A. Farley. 1994. The influence of β subunit structure on the stability of Na^+/K^+-ATPase complexes and interaction with K^+. *J. Biol. Chem.* 269:6550–6557.

Eraso, P., and C. Gancedo. 1987. Activation of yeast plasma membrane ATPase by acid pH during growth. *FEBS (Fed. Eur. Biochem. Soc.) Lett.* 224: 187–192.

Eraso, P., and F. Portillo. 1994. Molecular mechanism of regulation of yeast plasma membrane H^+-ATPase by glucose. *J. Biol. Chem.* 269:10393–10399.

Gaber, R. F. 1992. Molecular genetics of yeast ion transport. *Int. Rev. Cytol.* 137:299–353.

Garcia-Arranz, M., A. M. Maldonado, M. J. Mazon, and F. Portillo. 1994. Transcriptional control of yeast plasma membrane H^+-ATPase by glucose. *J. Biol. Chem.* 269:18076–18082.

Gething, M.-J., and J. Sambrook. 1992. Protein folding in the cell. *Nature*

(Lond.). 355:33–45.
Gietz, D., A. St. Jean, R. A. Woods, and R. H. Schiestl. 1992. Improved method for high efficiency transformation of intact yeast cells. *Nucleic Acids Res.* 20:1425.
Harris, S. L., S. Na, X. Zhu, D. Seto-Young, D. S. Perlin, J. H. Teem, and J. E. Haber. 1994. Dominant lethal mutations in the plasma membrane H^+-ATPase gene of *Saccharomyces cerevisiae*. *Proc. Natl. Acad. Sci. USA.* 91:10531–10535.
Higgins, D. G., and P. M. Sharp. 1989. Fast and sensitive multiple sequence alignments on a microcomputer. *Comput. Appl. Biosci.* 5:151–153.
Hoffman, C. S., and F. Winston. 1987. A ten-minute DNA preparation from yeast efficiently releases autonomous plasmids for transformation of *Escherichia coli*. *Gene (Amst.)*. 57:267–272.
Jaunin, P., F. Jaisser, A. T. Beggah, K. Takeyasu, P. Mangeat, B. C. Rossier, J.-D. Horisberger, and K. Geering. 1993. Role of the transmembrane and extracytoplasmic domain of β subunits in subunit assembly, intracellular transport, and functional expression of Na,K-pumps. *J. Cell Biol.* 123: 1751–1759.
Jones, E. 1991. Three proteolytic systems in the yeast *Saccharomyces cerevisiae*. *J. Biol. Chem.* 266:7963–7966.
Klausner, R. D. 1989. Sorting and traffic in the central vacuolar system. *Cell.* 57:703–706.
Klausner, R. D., and R. Sitia. 1990. Protein degradation in the endoplasmic reticulum. *Cell.* 62:611–614.
Kunkel, T. A., J. D. Roberts, and R. A. Zakour. 1987. Rapid and efficient site-specific mutagenesis without phenotypic selection. *Methods Enzymol.* 154: 508–519.
Kuo, M.-H., and E. Grayhack. 1994. A library of yeast genomic MCM1 binding sites contains genes involved in cell cycle control, cell wall and membrane structure, and metabolism. *Mol. Cell Biol.* 14:348–359.
Ljungdahl, P. O., C. J. Gimeno, C. A. Styles, and G. R. Fink. 1992. SHR3: a novel component of the secretory pathway specifically required for localization of amino acid permeases. *Cell.* 71:463–478.
Marcusson, E. G., B. F. Horazdovsky, J. L. Cereghino, E. Gharakhanian, and S. D. Emr. 1994. The sorting receptor for yeast vacuolar carboxypeptidase Y is encoded by the VPS10 gene. *Cell.* 77:579–586.
McCracken, A. A., and K. B. Kruse. 1993. Selective protein degradation in the yeast exocytic pathway. *Mol. Biol. Cell.* 4:729–736.
Minami, Y., A. M. Weissman, L. E. Samelson, and R. D. Klausner. 1987. Building a multichain receptor: synthesis, degradation, and assembly of the T-cell antigen receptor. *Proc. Natl. Acad. Sci. USA.* 84:2688–2692.
Musil, L. S., and D. A. Goodenough. 1993. Multisubunit assembly of an integral plasma membrane channel protein, gap junction connexon43, occurs after exit from the ER. *Cell.* 74:1065–1077.
Nothwehr, S. F., C. J. Roberts, and T. H. Stevens. 1993. Membrane protein retention in the yeast Golgi apparatus: dipeptidyl aminopeptidase A is retained by a cytoplasmic signal containing aromatic residues. *J. Cell Biol.* 121:1197–1209.
Nothwehr, S. F., and T. H. Stevens. 1994. Sorting of membrane proteins in the yeast secretory pathway. *J. Biol. Chem.* 269:10185–10188.
Novick, P., S. Ferro, and R. Schekman. 1981. Order of events in the yeast secretory pathway. *Cell.* 25:461–469.
Pfeffer, S., and J. E. Rothman. 1987. Biosynthetic protein transport and sorting by the endoplasmic reticulum and Golgi. *Annu. Rev. Biochem.* 56:829–852.
Raths, S., J. Rohrer, F. Crausaz, and H. Riezman. 1993. *end3* and *end4*: Two mutants defective in receptor-mediated and fluid-phase endocytosis in *Saccharomyces cerevisiae*. *J. Cell Biol.* 120:55–65.
Renaud, K. J., E. M. Inman, and D. M. Fambrough. 1991. Cytoplasmic and transmembrane domain deletions of Na,K-ATPase β-subunit. *J. Biol. Chem.* 266:20491–20497.
Riles, L., J. E. Dutchik, A. Baktha, B. K. McCauley, E. C. Thayer, M. P. Leckie, V. V. Braden, J. E. Depke, and M. V. Olson. 1993. Physical maps of the six smallest chromosomes of *Saccharomyces cerevisiae* at a resolution of 2.6 kilobasepairs. *Genetics.* 134:81–150.
Roberts, C. J., S. F. Nothwehr, and T. H. Stevens. 1992. Membrane protein sorting in the yeast secretory pathway: evidence that the vacuole may be the default compartment. *J. Cell Biol.* 119:69–83.
Rose, M. D., F. Winston, and P. Hieter. 1990. Methods in Yeast Genetics. Cold Spring Harbor Laboratory Press, Cold Spring Harbor, NY. 198 pp.
Sanger, F. S., S. Nicklen, and A. R. Coulson. 1977. DNA sequencing with chain-terminating inhibitors. *Proc. Natl. Acad. Sci. USA.* 74:5463–5467.
Serrano, R., B. M. Kielland, and G. R. Fink. 1986. Yeast plasma membrane ATPase is essential for growth and has homology with (Na^+,K^+), K^+-, and Ca^{2+}-ATPases. *Nature (Lond.)*. 319:689–693.
Sherman, F., J. B. Hicks, and G. R. Fink. 1986. Methods in Yeast Genetics. Cold Spring Harbor Laboratory Press, Cold Spring Harbor, NY. pp. 523–585.
Shinde, U., Y. Li, S. Chatterjee, and M. Inouye. 1993. Folding pathway mediated by an intramolecular chaperone. *Proc. Natl. Acad. Sci. USA.* 90: 6924–6928.
Sikorski, R. S., and P. Hieter. 1989. A system of shuttle vectors and yeast host strains designed for efficient manipulation of DNA in *Saccharomyces cerevisiae*. *Genetics.* 122:19–27.
Simons, K., and A. Wandinger-Ness. 1990. Polarized sorting in epithelia. *Cell.* 62:207–210.
Stack, J. H., and S. D. Emr. 1993. Genetic and biochemical studies of protein sorting to the yeast vacuole. *Curr. Opin. Cell Biol.* 5:641–646.
Steck, T. L., and J. Yu. 1973. Selective solubilization of proteins from red blood cell membranes by protein perturbants. *J. Supramol. Struct.* 1:220–232.
Trowbridge, I. S., J. F. Collawn, and C. R. Hopkins. 1993. Signal-dependent membrane protein trafficking in the endocytic pathway. *Annu. Rev. Cell Biol.* 9:129–161.
Welsh, M. J., and A. E. Smith. 1993. Molecular mechanisms of CFTR chloride channel dysfunction in cystic fibrosis. *Cell.* 73:1251–1254.